2012

Modulation of the pHLIP Transmembrane Helix Insertion Pathway

Alexander G Karabadzhak
University of Rhode Island

Dhammika Weerakkody

See next page for additional authors

Citation/Publisher Attribution

Karabadzhak A.G., Weerakkody D., Wijesinghe D., Thakur M.S., Engelman D.M., Andreev O.A., Markin V.S., Reshetnyak Y.K. (2012). Modulation of the pHLIP transmembrane helix insertion pathway, *Biophysical Journal,* 102(8) ,1846-1855.
Available at: http://dx.doi.org/10.1016/j.bpj.2012.03.021

Modulation of the pHLIP Transmembrane Helix Insertion Pathway

Alexander G. Karabadzhak,[†] Dhammika Weerakkody,[†] Dayanjali Wijesinghe,[†] Mak S. Thakur,[†] Donald M. Engelman,[‡] Oleg A. Andreev,[†] Vladislav S. Markin,[§] and Yana K. Reshetnyak[†*]

[†]Physics Department, University of Rhode Island, Kingston, Rhode Island; [‡]Department of Molecular Biophysics and Biochemistry, Yale University, New Haven, Connecticut; and [§]Department of Neurology, University of Texas Southwestern Medical Center, Dallas, Texas

ABSTRACT The membrane-associated folding/unfolding of pH (low) insertion peptide (pHLIP) provides an opportunity to study how sequence variations influence the kinetics and pathway of peptide insertion into bilayers. Here, we present the results of steady-state and kinetics investigations of several pHLIP variants with different numbers of charged residues, with attached polar cargoes at the peptide's membrane-inserting end, and with three single-Trp variants placed at the beginning, middle, and end of the transmembrane helix. Each pHLIP variant exhibits a pH-dependent interaction with a lipid bilayer. Although the number of protonatable residues at the inserting end does not affect the ultimate formation of helical structure across a membrane, it correlates with the time for peptide insertion, the number of intermediate states on the folding pathway, and the rates of unfolding and exit. The presence of polar cargoes at the peptide's inserting end leads to the appearance of intermediate states on the insertion pathway. Cargo polarity correlates with a decrease of the insertion rate. We conclude that the existence of intermediate states on the folding and unfolding pathways is not mandatory and, in the simple case of a polypeptide with a noncharged and nonpolar inserting end, the folding and unfolding appears as an all-or-none transition. We propose a model for membrane-associated insertion/folding and exit/unfolding and discuss the importance of these observations for the design of new delivery agents for direct translocation of polar therapeutic and diagnostic cargo molecules across cellular membranes.

INTRODUCTION

The molecular mechanism of spontaneous polypeptide folding and insertion into a membrane, as well as its exit and unfolding, is of interest from several standpoints, including the action of antimicrobial peptides, the folding and degradation of membrane proteins, and the medical applications of the pH-triggered insertion peptides. Most helical membrane proteins insert into a lipid bilayer with the assistance of the translocon machinery (1,2). Although they are assisted in their pathways by the Get proteins (3), tail-anchored membrane proteins can spontaneously insert and fold themselves across the lipid bilayer of a membrane and may do so when released by the Get complex in vivo (4,5). The stability and folding of membrane proteins are strongly constrained by the formation of secondary structures in the lipid bilayer environment, driven by the hydrophobic effect and hydrogen bonding (6–8). When helical membrane proteins are degraded, their transmembrane (TM) helices must exit the bilayer as they become destabilized by cleavages (9). Peptide insertion into a bilayer can be triggered by a pH jump if it leads to the protonation/deprotonation of charged groups to render them uncharged and so to increase peptide hydrophobicity and affinity for the nonpolar region of a membrane. One example of a synthetic peptide with pH dependent membrane-insertion properties has been investigated by White and Ladokhin (10). Another example, which is the subject of this study, is the pHLIP family. At neutral and high pH, pHLIP is monomeric and largely unstructured, and equilibrates between aqueous solution and the surface of a lipid bilayer. Lowering the pH shifts the equilibrium toward transmembrane insertion and the formation of a TM helix (11). A subsequent increase of pH promotes unfolding of the TM helix and exit from the bilayer. The process of binding of the peptide to the membrane surface is accompanied by an energy release of 6–7 kcal/mol and the process of insertion is accompanied by an additional energy release of ~1.8–2.0 kcal/mol (12). We previously showed that pHLIP insertion is associated with the protonation of Asp/Glu residues, which leads to an increase of hydrophobicity that triggers the folding and insertion of the peptide across a lipid bilayer (13,14). The insertion of the pHLIP is unidirectional: the C-terminus crosses the lipid bilayer, and the N-terminus stays outside (11,15). The energy of membrane-associated folding can be used to favor the movement of cell-impermeable polar cargo molecules across the hydrophobic membrane bilayer when they are attached to the inserting end of the pHLIP (15–17). Both pH-targeting behavior and molecular translocation have been demonstrated in cultured cells and in vivo (16–21). Thus, there is an opportunity to develop a novel concept in drug delivery, which is based on the use of a monomeric, pH-sensitive peptide molecular transporter to deliver agents that are significantly more polar than conventional drugs.

In our initial kinetic study, we found that pHLIP inserts into a POPC phospholipid bilayer in several steps: first, an

Submitted September 26, 2011, and accepted for publication March 12, 2012.

*Correspondence: reshetnyak@mail.uri.edu

Editor: William Wimley.

0006-3495/12/04/1846/10 $2.00

doi: 10.1016/j.bpj.2012.03.021

interfacial helix is rapidly formed (~100 ms), followed by slow transmembrane insertion (~1 min) along a pathway that contains several intermediates. The exit of the peptide from the bilayer core proceeds ~800 times faster and through different intermediates (22). Questions that remain unanswered from that study are why it takes 1000 times longer for the helix to insert across a bilayer after it is formed on the surface, and what the intermediates are on the insertion/exit pathways. Another question we want to address is how polar cargo might affect the process of peptide insertion and thus translocation of the cargo across the bilayer.

MATERIALS AND METHODS

Due to space limitations, the detailed description of experiments can be found in the Supporting Material.

RESULTS

Design of pHLIP variants

Our previous data indicate that the pHLIP forms a helix, after a pH drop, 1000 times faster than it inserts into a lipid bilayer, and insertion occurs through several steps. The insertion time and nature of the intermediates might result from the presence of four protonatable groups at the C-terminus of the peptide, which have to cross the membrane to complete the process of insertion. To cross the energy barrier presented by the hydrophobic membrane core at any appreciable rate, it is reasonable to hypothesize that these charged groups should be at least partially protonated. To test the idea, we asked whether the number of protonatable groups at the C-terminus would correlate with the rates of insertion and exit, and examined as well the number of intermediate states along the insertion/exit pathways. Two truncated pHLIP variants were designed: pHLIP-2 and pHLIP-1, where the number of protonatable groups (shown below in bold print) was reduced to two and one, respectively. Additional Asp residues were placed at the N-terminus to preserve peptide solubility.

pHLIP-4, AE–QN–PI YWARYADWLFTTPLLLLDLA LLV **DADE**GT**COOH**
pHLIP-2, AEDQN–P– YWARYADWLFTTPLLLLDL ALLV **D** – – – G–**COOH**
pHLIP-1, AEDQNDP– YWARYADWLFTTPLLLLDL ALLV – – – –G–**COOH**

To gain insight into the structural nature of the intermediates along the insertion and exit pathways, we studied three single-Trp variants of pHLIP-4 peptide (pHLIP-W1, pHLIP-W2, and pHLIP-W3), where a Trp residue was positioned at the beginning, middle, and end of the TM helix.

pHLIP-W1, AEQNPI Y**W**ARYADFLFTTPLLLLDLA LLV DADET-COOH
pHLIP-W2, AEQNPI YFARYAD**W**LFTTPLLLLDLA LLV DADET-COOH
pHLIP-W3, AEQNPI YFARYADFLFTTPLLLLDLA LL**W** DADET-COOH

The following pHLIP sequences were selected for the conjugation of polar cargoes to the inserting end to probe cargo effects on kinetics:

pHLIP-4, AE–QN–PI YWARYADWLFTTPLLLLDLA LLV **DADE**GCT**COOH**
pHLIP-2, AEDQN–PI YWARYADWLFTTPLLLL**D**LA LLV **D** – – – GCT**COOH**
pHLIP-2E, AEDQNDPI YWARYADWLFTTPLLLL**E**L ALLV **E** – – – GCT**COOH**

pHLIP-2E is a pHLIP-2 where the two Asp residues are replaced by Glu to increase the pKa of peptide insertion, which is desirable for the translocation of polar cargo into the cytoplasm. Each of the last three pHLIP variants had a free SH group at its C-terminus for conjugation with maleimide-cargo. We chose as cargo biotin and biotin-Peg, mainly based on their log *P* values (chosen to be slightly polar), the convenience of conjugation to the peptides, the low level of absorbance, and the absence of fluorescence in the ultraviolet range (in contrast to fluorescent dyes and phallatoxins). The measured log *P* values of biotin-maleimide and biotin-Peg-maleimide are −0.3 and −1.4, respectively (for comparison, the log *P* values of phalloidin-rhodamine and phalloidin are −0.05 and −1.5, respectively (16). Information about Log *P* measurements can be found in the supporting material. We have shown previously that pHLIP-4 is capable of translocating biotin-Peg (23). All constructs were purified to remove unreacted peptide and cargo.

Steady-state study of pHLIP variants

We employed fluorescence and CD/OCD spectroscopic techniques to demonstrate that pHLIP variants and their cargo conjugates preserve pH-dependent membrane-inserting properties (Fig. S1, Fig. S2, Fig. S3, and Fig. S4 in the Supporting Material). The data clearly indicate that all peptides preserve the ability to interact with the lipid bilayer of the membrane in a pH-dependent manner. The data also suggest that the peptides may be partly pulled away from the membrane core by the polar cargo molecules attached to their C-termini (especially pHLIP-2 and pHLIP-2E, which are more hydrophobic, partition more deeply into the membrane, and have higher helix content at pH 8 compared to pHLIP-4) (Fig. S3 and Table S1). Because we had moved protonatable residues from the C- to the N-terminus and attached polar (noncharged) cargo, we checked for effects on the pH dependency of the insertion (Fig. S1, *c* and *f,* and Fig. S4). The perturbation of the insertion pKa by truncation of the C-terminus and attachment of the polar cargoes is small.

Mathematical models for fitting of kinetics data

In our earlier kinetic studies, we used a sequential mathematical model to fit the kinetic data and to find the rates and contributions of individual components (22). To simplify the mathematical model, only forward reactions were taken into consideration. In this work we have made an attempt to describe the processes by taking into account both forward and backward reactions. We have considered several linear models: two-state (no intermediates),

$$\mathrm{A} \underset{k_1^-}{\overset{k_1}{\rightleftarrows}} \mathrm{B},$$

three-state (a single intermediate),

$$\mathrm{A} \underset{k_1^-}{\overset{k_1}{\rightleftarrows}} \mathrm{B} \underset{k_2^-}{\overset{k_2}{\rightleftarrows}} \mathrm{C},$$

and four-state (two intermediates) models,

$$\mathrm{A} \underset{k_1^-}{\overset{k_1}{\rightleftarrows}} \mathrm{B} \underset{k_2^-}{\overset{k_2}{\rightleftarrows}} \mathrm{C} \underset{k_3^-}{\overset{k_3}{\rightleftarrows}} \mathrm{D}.$$

The transitions between states are described by a set of differential equations (Appendices S1–S3), which can be solved, but the functions obtained are very complex and will contain a number of variable parameters increasing with the complexity of the applied model. It is not practical to perform fitting of the experimental data using such complex functions: a slight variation in input data dramatically affects the solution, thus making it unreliable. However, the solution for fluorescence variation with time can be presented in a general form as a sum of the exponential functions:

$$F(t) = f_0 + f_1 \exp\left(\frac{-t}{\tau_1}\right) \tag{1}$$

for the two-state model;

$$F(t) = f_0 + f_1 \exp\left(\frac{-t}{\tau_1}\right) + f_2 \exp\left(\frac{-t}{\tau_2}\right) \tag{2}$$

for the three-state model, and

$$F(t) = f_0 + f_1 \exp\left(\frac{-t}{\tau_1}\right) + f_2 \exp\left(\frac{-t}{\tau_2}\right) + f_3 \exp\left(\frac{-t}{\tau_3}\right) \tag{3}$$

for the four-state model, where τ_i is the characteristic time for each transition, $\nu_i = 1/\tau_i$ is the characteristic rate of transition, and f_i is the characteristic contribution. Thus, fitting of the measured curves can be performed using exponential functions and the characteristic rate constants, ν_i, can be found directly from the experiment. However, we wish to emphasize that the characteristic rates (or times) and contributions need to be related to the rate constants (k_i) and contributions for the transition from one intermediate to another, which fully reflect the transitions. Due to the complexity of the problem, we proposed to establish relations only between the characteristic rates and the real rate constants, without considering the contributions. By making a few reasonable assumptions, simple approximate relations between k and ν can be established. Thus, for the two-state model (see Appendix S1 in the Supporting Material),

$$k_1 \sim 0.91\nu_1; \tag{4}$$

for the three-state model (see Appendix S2 in the Supporting Material),

$$k_1 \sim \frac{\nu_1}{1.1} - \frac{\nu_2}{12.21}, \quad k_2 \sim 1.0091\nu_2; \tag{5}$$

and for the four-state model (see Appendix S3 in the Supporting Material),

$$k_1 \sim \nu_1, \quad k_2 \sim \frac{\nu_2}{1.1} - \frac{\nu_3}{12.21}, \quad k_3 \sim 0.991\nu_3. \tag{6}$$

The experimental kinetic data were fitted by the single, double, or triple exponential functions (Eqs. 1–3), which are general solutions for the two-, three-, or four-state models, respectively.

Kinetics of insertion of pHLIP variants with truncated C-termini at various temperatures

The insertion of pHLIP-4, -2, and -1 into a lipid bilayer was in each case triggered by a drop in pH from 8 to 3.6 and was monitored at various temperatures (7, 11, 18, and 25°C) by the increase of tryptophan fluorescence (Fig. 1, *a–c*). pHLIP-4 inserts across the bilayer as a helix within 30–50 s (at various temperatures), pHLIP-2 within 3–8 s, and pHLIP-1 within 80–400 ms, which is about the same as the time of helix formation (90–100 ms) (Table 1). Thus, the processes of helix formation and insertion occur practically simultaneously in the absence of protonatable side chains at the C-terminal tail, and the number of protonatable residues at the inserting end does not affect the formation of helical structure, but correlates with the time of peptide insertion into the lipid bilayer.

To ensure that the addition of Asp residues to the N-terminus of truncated pHLIP variants does not alter the kinetics, we tested the sequence

pHLIP-6, AEDQNDPIYWARYADWLFTTPLLLLDLALLVDADEGTCOOH,

where an additional two Asp residues (total of six Asp residues) were placed at the N-terminus of pHLIP-4. The steady-state and kinetics data obtained for pHLIP-6 were

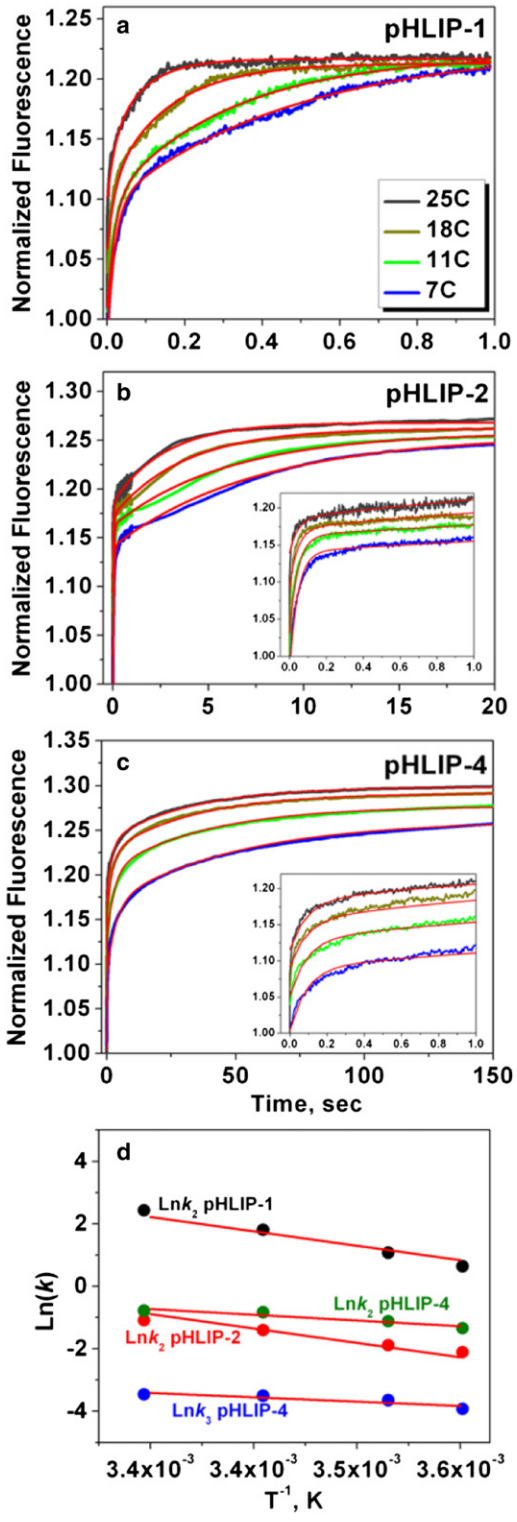

FIGURE 1 Insertion kinetics of pHLIP-4, -2, and -1 at different temperatures, with Arrhenius plots shown for the second and third rates. The data were fitted by the Arrhenius equation. Fitting curves are in red.

very similar to the data obtained with pHLIP-4 (Fig. S5), confirming our suggestion that the modification of the N-terminus does not interfere with the process of insertion.

TABLE 1 Insertion at different temperatures

	25°C	18°C	11°C	7°C
pHLIP-1	0.02 (44.4–45.3) for various temperatures			
	0.08 (12.6)	0.15 (6.72)	0.31 (3.26)	0.48 (2.10)
pHLIP-2	0.04 (22.70–22.72) for various temperatures			
	2.7 (0.37)	3.7 (0.27)	6.0 (0.17)	7.5 (0.13)
pHLIP-4	0.09 (11.1) for various temperatures			
	2.0 (0.45)	2.1 (0.43)	2.8 (0.32)	3.5 (0.26)
	32 (0.031)	33 (0.030)	38 (0.026)	50 (0.020)

Characteristic times, τ (s), and rate constants, k (s^{-1}) (in parentheses) are shown. For each pHLIP variant, the data columns, reading across, contain kinetics parameters for the fastest, slow, and slowest transitions, respectively.

Activation energies of pHLIP-variant insertion into bilayer

Arrhenius plots were constructed to establish activation energies (E_a) and frequency factors (A) for the transitions between the states for each pHLIP variant (Fig. 1 *d*). The points were fitted by the Arrhenius equation

$$\ln k = \frac{-E_a}{RT} + \ln A. \quad (7)$$

A global fit was used in the analysis of the second transition for pHLIP-2 and -1, and of the second and third transitions for pHLIP-4, since slopes of the corresponding curves are very similar to each other (established by separate fitting of each data set). In the global fitting we used activation energy as a shared parameter to establish differences in the frequency factors for various transitions. The activation energy barrier for pHLIP-1 and -2 is 13.2 kcal/mol. The frequency factor for the pHLIP-1 transition to the final state is 4.2×10^{10}, which is an order of magnitude higher than the frequency factor for pHLIP-2 (1.9×10^{9}): we reason that this finding may reflect the lower probability of simultaneous protonation of both COO^- groups of Glu and C-terminus on pHLIP-2, relative to the probability of protonation of the single carboxyl terminus of pHLIP-1. Insertion of the helical structure of pHLIP-4 into the lipid bilayer occurs in two steps, with an activation barrier of ~4.6 kcal/mol each (9.2 kcal/mol combined), but with frequency factors (1.1×10^{3} for B→C transition) more than a million times lower than for pHLIP-2 and -1. An especially low frequency factor of 80 (for the C→D transition) was obtained for the transition to the final TM state for pHLIP-4.

Kinetics of insertion of pHLIP variants with cargoes

The attachment of biotin or biotinPeg cargoes to the peptides slows down the process of insertion. The overall insertion time of pHLIP-4 increases from 30–35 s to 400 s and 500 s, when biotin and biotin-Peg, respectively, are attached to the inserting ends (Fig. 2 and Table 2). For

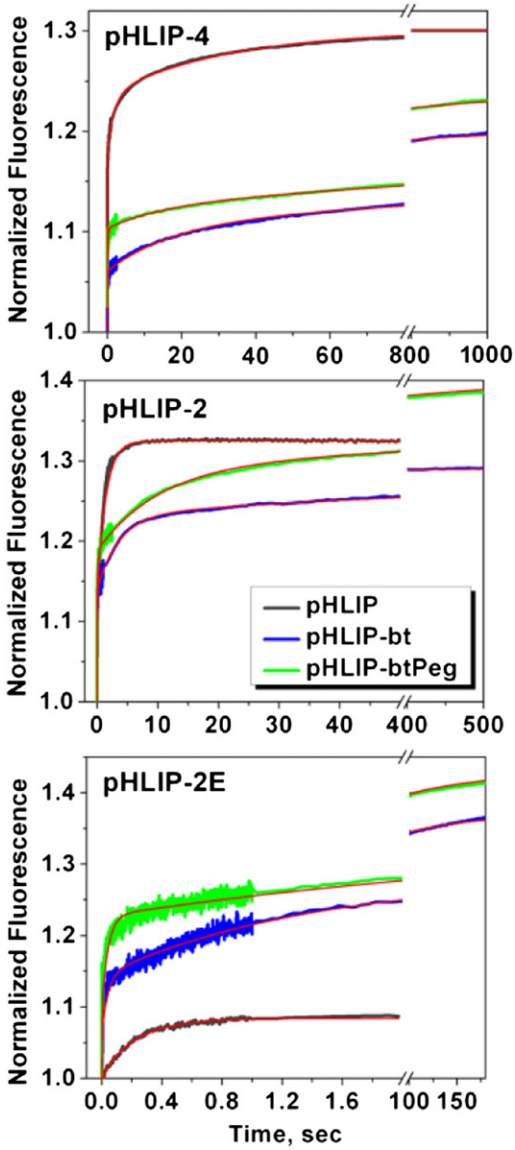

FIGURE 2 Insertion of pHLIP-4, -2, and -2E with no cargo and with biotin and biotinPeg cargoes attached to the inserting ends of the peptides. The fitting curves are in red.

pHLIP-2 and pHLIP-2E, the processes of insertion slow from 1–2 s to 100–200 s, and from 0.2 s to 80–90 s with the addition of biotin and biotin-Peg, respectively. At the same time, the first (fast) rate of the insertion is very similar for all pHLIP variants with and without cargo, and it coincides with the rate of helix formation. The higher the polarity of the cargo attached to the inserting end, the slower the final steps to adopt TM orientation and flip cargo across a membrane. It is interesting to note that the biggest change of the fluorescence signal for pHLIP-4 is observed for the peptide with no cargo. The steady-state measurements (Fig. S3) indicate that state II (membrane-bound) is not affected significantly by the attachment of cargoes. At the same time, when cargoes are attached, fewer pHLIP-4 peptides are reaching state III (TM orientation) and smaller changes in the fluorescence signal are observed. In contrast to pHLIP-4, in the cases of pHLIP-2, and especially pHLIP-2E, the increase of fluorescence is higher for peptides with cargo compared to peptides with no cargo. Truncated pHLIP-2s partition more deeply into the membrane and are already exhibiting formation of elements of secondary structure in state II, which is reflected by the shift in maximum position of the fluorescence spectrum and the increase in emission (Table S1). The cargo pulls the peptides to the membrane surface, affecting their state II positions. Thus, pHLIP-2 and pHLIP-2E with cargo start their journeys into the membrane to adopt the TM configuration from a more superficial membrane surface configuration compared to peptides with no cargo, which are more membrane-embedded at high and neutral pH.

TABLE 2 Insertion with cargoes

	No cargo	Biotin	Biotin-Peg
pHLIP-4	0.07–0.15 (14.2–6.7) for various cargo		
	2 (0.45)	17 (0.05)	16 (0.05)
	32 (0.03)	385 (0.0026)	416 (0.0024)
pHLIP-2	0.1–0.6 (10–1.7) for various cargo		
	2.7 (0.37)	3.6 (0.25)	10.0 (0.09)
	—	102 (0.0097)	253 (0.0039)
pHLIP-2E	0.04 (22–25) for various cargo		
	0.2 (0.45)	1.4 (0.65)	3.4 (0.27)
	—	80 (0.012)	90 (0.011)

Characteristic times, τ (s), and rate constants, k (s^{-1}) (in parentheses) are shown. For each pHLIP variant, the three columns of data, reading left to right, contain kinetics parameters for the fastest, slow, and slowest transitions, respectively.

Insertion/folding transitions to intermediate pH

To further study the intermediate states of insertion, we compared transitions from pH 8 to 3.6 and intermediate pH (pH 8→6, pH 8→5) (Fig. S6). When the size of the pH jump is reduced, both peptide folding and bilayer insertion slow down. The first (fast) rate of the insertion is very similar for all pHLIP variants (Table 3), and it coincides with the rate of helix formation; however, after the first 100–300 ms, the behavior of the pHLIP variants is significantly different. pHLIP-1 forms a helical structure and partitions into the lipid bilayer slightly more slowly when the pH is jumped from 8 to 6 than when it is jumped from 8 to 3.6. All processes are completed within the first 200–300 ms for pHLIP-1 at any pH jump. It appears that the absence of several protonatable groups at the inserting end makes the peptide less dependent on the variations in pH jump. In contrast, pHLIP-2 and pHLIP-4 insertions into the membrane are more dependent on the final pH. Thus, the more protonatable groups there are on the inserting end, the slower is the process of insertion at the intermediate pH jumps. Interestingly, ~85% of the CD signal changes

TABLE 3 Insertion and folding at different pH transitions

	pH 8→3.6	pH 8→5	pH 8→6
pHLIP-1 fluoresc.	0.02 (44.6–45.0) for various pHs		
	0.09 (10.3)	0.18 (5.6)	0.20 (5.0)
pHLIP-1, CD	0.09 (10.1) for various pHs		
pHLIP-2 fluoresc.	0.08 (11.3–11.4) for various pHs		
	2.8 (0.36)	4.5 (0.22)	13.0 (0.08)
pHLIP-2, CD	0.08 (11.3–11.4) for various pHs		
	2.2 (0.46)	5.0 (0.20)	13.0 (0.08)
pHLIP-4 fluoresc.	0.09 (11.1) for various pHs		
	2.0 (0.45)	3.4 (0.27)	**5.0 (0.18)**
	32 (0.031)	102 (0.0097)	138 (0.0072)
pHLIP-4, CD	0.09 (11.1) for various pHs		
	2.0 (0.45)	5.0 (0.18)	**5.0 (0.18)**
	32 (0.031)	102 (0.0097)	138 (0.0072)

Characteristic times, τ (s), and rate constants, k (s^{-1}) (in parentheses) are shown. For each pHLIP variant, the three columns of data, reading left to right, contain kinetics parameters for the fastest, slow, and slowest transitions, respectively.

for both peptides occur within the first 80 ms for all pH transitions, whereas the rate constants for the remaining 15% of the CD signal changes correlate very well with the rate constant of the fluorescence changes at the final step of insertion and depend on the pH-jump magnitude. It seems that the final adjustment of the content of helical structure occurs at the final stage of insertion, when the peptides adopt TM orientations.

We observed an interesting behavior of pHLIP-4 when the pH was dropped from 8 to 6, and a kink appeared in the fluorescence and CD kinetic curves (Fig. 3). The kinetic curves of the insertion and folding at the pH 8→6 jump were fitted by three-exponential functions with negative amplitudes for the second component (Table 3, *bold print*). The physical meaning of a negative amplitude is that the spectral signal changes in the opposite direction. These changes indicate that after the pH is dropped, pHLIP-4 first partitions into the lipid bilayer with a helical structure formation but later comes out of the membrane with a reduction in helical content and then finally dives slowly into the membrane with an increase in helical content.

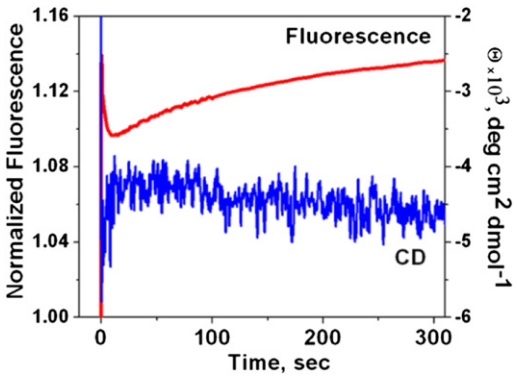

FIGURE 3 Kink in the fluorescence and CD kinetic curves at the pH 8→6 transition for the pHLIP-4 variant.

Exit/unfolding of pHLIP variants

We also investigated the reverse processes of exit/unfolding of the pHLIP variants when the pH is changed from 3.6 to 6, 7, and 8 (Fig. S7 and Table 4). Our CD and fluorescence data show very fast, 50- to 150-ms exit transitions for each variant when the pH is raised to 8. With a reduction in the size of the pH jump, both unfolding and exit from the bilayer slow down. As in the case of insertion/folding, the pHLIP-1 kinetics is less sensitive than that of pHLIP-2 or -4 to the magnitude of the pH jump. Exit/unfolding of pHLIP-2 slows down from 200 ms for a pH 3.6→8 jump to 60–80 s for a pH 3.6→6 jump. Dramatic changes are observed for pHLIP-4 with different pH jumps: the exit/unfolding slows down from 200 ms to 150–170 s.

Insertion/folding and exit/unfolding of single-Trp pHLIP variants

Wishing to better understand the intermediates, we used tryptophan residues positioned along the sequence to follow insertion and exit of different parts of pHLIP-4 into and out of a lipid bilayer (Fig. 4 and Table 5). The characteristic times of the transitions for the single-Trp variants are similar to those of pHLIP-4, whereas double the time is required for pHLIP-W2 and -W3 to insert and adopt their final TM configurations when the pH is dropped from 8 to 3.6. For the pH 8→6 transition, a kink is observed similar to that seen for pHLIP-4 within the same timescale of 4–7 s. The most pronounced kink is observed for pHLIP-W3, and less pronounced kinks are seen for pHLIP-W1 and -W2. As mentioned above, the kink is interpreted as a partial exit and unfolding of pHLIP-4 in the path to the inserted and folded state when the pH is dropped from 8 to 6. Based on this view, we infer that the C-terminal end of the peptide, which has four protonatable groups, tends to exit the bilayer to a greater extent than other parts of the peptide.

Exit and unfolding for the pH 3.6→8 transition happens quickly for all single-Trp variants (within 350 ms), but

TABLE 4 Exit and unfolding at different pH transitions

	pH 3.6→8	pH 3.6→7	pH 3.6→6
pHLIP-1 fluoresc.	0.14 (7.14)	0.40 (2.5)	0.85 (1.18)
pHLIP-1, CD	0.02 (45.5) for various pHs		
pHLIP-2 fluoresc.	0.03(29.9)	0.3 (3.01)	8.1 (0.11)
	0.21 (4.81)	4.8 (0.21)	67.7 (0.015)
pHLIP-2, CD	0.02 (50)	0.3 (3.01)	8.0 (0.11)
		3.9 (0.26)	77.0 (0.013)
pHLIP-4 fluoresc	0.03 (29.9)	0.22 (4.12)	16.8 (0.054)
	0.2 (5.05)	11 (0.092)	175 (0.0058)
pHLIP-4 CD	0.02 (50)	0.22 (4.12)	16.8 (0.054)
		6.5 (0.16)	149 (0.0068)

Characteristic times, τ (s), and rate constants, k (s^{-1}) (in parentheses) are shown. For each pHLIP variant, the three columns of data, reading left to right, contain kinetics parameters for the fastest, slow, and slowest transitions, respectively.

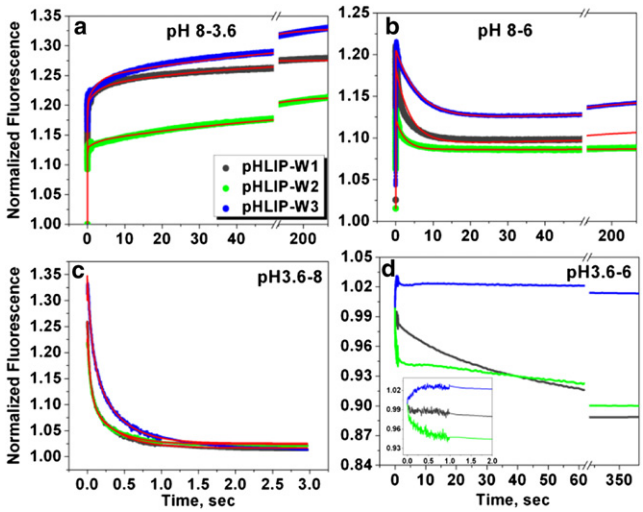

FIGURE 4 Insertion/exit of single-Trp pHLIP variants at different pHs. The fitting curves are in red.

much more slowly for the intermediate transition driven by the pH 3.6→6 jump. (Fig. 4, *c* and *d*). Interesting changes were observed for pHLIP-W3 with a pH increase from 3.6 to 6: although the fluorescence decays progressively for pHLIP-W1 and -W2, pHLIP-W3 exhibits an initial increase of fluorescence, which then decays slowly. Our interpretation is that the changes are related to the movement of Trp residues across the bilayer as the pHLIP-W3 peptide exits the membrane.

Rates of pH equilibration in POPC liposomes

It is known that the pH inside a liposome equilibrates progressively with the external pH after a pH jump (24). However, the rate of equilibration depends on the magnitude of the pH changes, the concentrations of other ions present, the charges on the lipid headgroups, the buffering capacities inside and outside the vesicles, and other factors. One of the widely used methods to follow changes is to monitor fluorescence changes of the pH-sensitive dye fluorescein (FITC) encapsulated in the liposomes. FITC carries two negative charges at pH 9 that are protonated as the pH is lowered. Since some of the charged residues of pHLIP peptides are located near the bilayer surfaces (on inner or outer leaflets), we chose to use lipid-bound FITC to probe pH changes near the inner leaflet rather than bulk pH changes. We followed pH equilibration after the addition of acid or base using liposomes containing 1% FITC-labeled phospholipids. Biphasic kinetics were seen for a pH jump from 8 to 3.6 with characteristic rates of ~0.04 and 0.003 s^{-1} (Fig. S8 *a*), data that are in a good agreement with the rates measured previously (25). Thus, the fastest component of the pH changes inside a liposome is of the same order of magnitude as the slowest component of pHLIP-4 insertion, whereas pHLIP-2, -2E, and -1 fold and insert into the lipid bilayer much faster than the pH equilibrates on the bilayer inner leaflet. In the case of a pH jump from 8 to 6, the first component slows down to 110 s (0.009 s^{-1}) and the second component is not detectable within 20 min.

We also measured the FITC fluorescence changes when the solution pH is raised from 3.6 to 8 and to 6 by addition of NaOH (the solution already contained H^+ and Cl^- ions to mimic our unfolding experiments). In both cases, the characteristic time of the first increase of FITC fluorescence associated with the pH changes on the inner leaflet of the bilayer is ~20 s (Fig. S8, *c* and *d*), after which it takes tens of minutes more for the pH to be fully equilibrated.

TABLE 5 Insertion and exit of single-Trp pHLIP variants at various pH transitions

	pHLIP-W1	pHLIP-W2	pHLIP-W3
pH 8→3.6	0.09 (11.1) for various pHLIPs		
		2.5 (0.36)	
	35 (0.028)	76 (0.013)	71 (0.014)
pH 8→6	0.01 (100) for various pHLIPs		
	4.0 (0.22)	2.6 (0.35)	6.2 (0.14)
	200 (0.005) for various pHLIPs		
pH 3.6→8	0.04 (22.5)	0.05 (18.0)	0.06 (14.9)
	0.35 (2.88) for various pHLIPs		
pH 3.6→6	4.2 (0.21)	—	—
	54.9 (0.02)	—	—

Characteristic times, τ (s), and rate constants, k (s^{-1}) (in parentheses) are shown. For each pHLIP variant, the three columns of data, reading left to right, contain kinetics parameters for the fastest, slow, and slowest transitions, respectively.

DISCUSSION

In this study, we designed several pHLIP variants and examined how elements of the pHLIP peptide and polar cargoes attached to the inserting end determine the pathways and kinetics of peptide insertion across and exit from a lipid bilayer. Based on our results, we have developed a model that describes our current view of the polypeptide membrane entry and exit pathways, as well as cargo translocation across the bilayer (Fig. 5). The model assumes a sequential pathway for the processes of insertion and exit, and takes state II as a starting point, where the peptide is bound to the surface of the lipid bilayer in a predominantly unstructured configuration. A drop of pH leads initially to protonation (or partial protonation) of the carboxyl groups located in the TM part of the peptide, which are positioned closer to the hydrophobic core of the bilayer and, most probably, have the highest values in the sequences for the pK_a of protonation, since the other titratable groups are not as constrained by nearby side-chain hydrophobicity to lie near the interface. It is known that the pK_a of the protonation/deprotonation of residues depends on the dielectric properties of their environment (26,27), and it was shown previously that buried Asp residues in the C-helix of

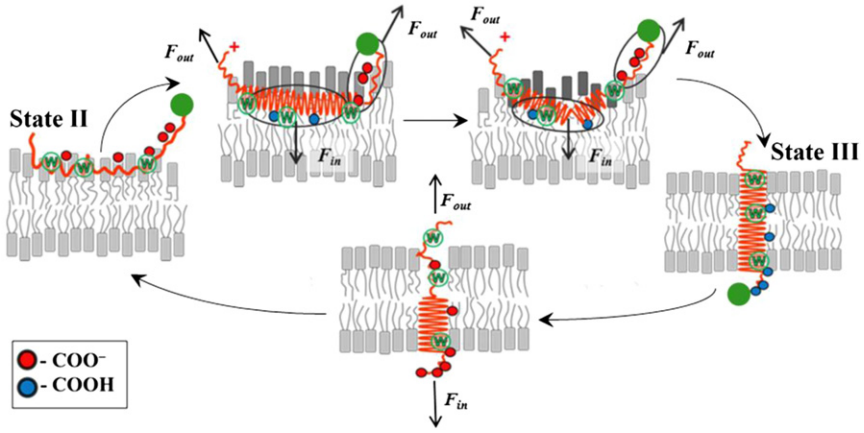

FIGURE 5 Model of membrane-associated folding and unfolding. The schematic presentation of the insertion/folding and exit/unfolding of pHLIP polypeptides. The letter W indicates approximate positions of Trp residues in the single-Trp pHLIP-4 variants. Small red and blue circles represent the approximate positions of the protonatable carboxyl groups of Asp, Glu, and the C-terminus. The green circle represents polar cargo attached to the inserting end of the peptide. Membrane distortion is shown schematically by lipids with darker headgroups. In the case of pHLIP peptides with no cargo and a nonprotonatable C-terminal end, the insertion and folding appears without intermediates as an all-or-none transition.

bacteriorhodopsin, from which pHLIP is derived, have higher pK_as of protonation than do those exposed to a more polar aqueous environment (28). Protonation of the carboxyl groups in the TM parts of pHLIP peptides induces a deeper penetration of the peptide into the membrane, which is accompanied by the formation of secondary structure within the first 20–90 ms, stabilized by the formation of internal H-bonds that result from the depletion of water in their environment. As a result, an effective force directed toward the bilayer core ($\vec{F}_{in}$) is created at the center of the TM region where the hydrophobic Leu and protonated Asp residues are located. On the other hand, at the negatively charged C-terminus (which most probably has not yet been protonated) and positively charged N-terminus, the net forces ($\vec{F}_{out}$) are directed away from the bilayer core. This force becomes even stronger if polar cargo is attached to the inserting end of the peptide. The difference in folding/insertion between pHLIP-4, -2, and -1 and peptides with and without polar cargoes corresponds to the strength of the force pulling these sequences away from the membrane, which is greatest for pHLIP-4 with cargo (pHLIP-4 itself has four charged groups at its C-terminus), and smallest for pHLIP-1, which has only its C-terminal carboxyl group. These forces account in part for the observation that the insertions of pHLIP-2 and -1 into a lipid bilayer are completed 10 and 100 times faster than the insertion of pHLIP-4, since they bias the position of the peptide away from the energy barrier that must be crossed. Moreover, the existence of a large pulling force at the C-terminus of pHLIP-4 may account for the stabilization of an additional intermediate on the insertion pathway, which is most probably transient in the case of pHLIP-2 and -1 insertions. In the case of the intermediate pH jump from 8 to 6, the probability of protonation of the C-terminal carboxyl groups is even lower, so the $\vec{F}_{out}$ force becomes more significant, which may lead to partial exit of the pHLIP-4 peptide from the bilayer and the reduction of helical content observed experimentally. Experiments with the single-Trp pHLIP-4 variants allowed us to demonstrate that the C-terminal part of the TM helix moves away from the membrane more than the N-terminal part does, whereas the middle of the TM helix does not move much.

The process of unfolding/exit is induced by a pH jump from acid to base, which most probably leads to the deprotonation (or at least partial deprotonation) of Asp residues located in the TM parts of the peptides. It results in the presence of charges that are unstable in the membrane interior, and an outward force appears. As a peptide exits from the bilayer, it progressively unfolds. We note that the folding/insertion experiments, which are performed on liposomes, may mimic the real processes of a polypeptide's interaction with cellular membranes quite well but have the shortcoming that the pH difference that is present across the plasma membrane of a living cell is absent. For a cell in a diseased tissue, the intracellular pH is ~7.2–7.4, whereas the extracellular pH is low. We expect that carboxyl groups translocated across a bilayer are in their noncharged form, since the pH is equilibrated inside liposomes. For a large pH jump, all pHLIP variants, regardless of the number of protonatable groups at their C-termini, exit and unfold at least 100 times faster than the pH starts to be equilibrated inside a liposome (~20 s), so the protonatable groups can make the journey before they see the higher pH inside the liposome. However, for the intermediate pH jumps, the probability of deprotonation of carboxyl groups in the TM part is much lower, and the pH inside the liposome starts to equilibrate faster (within 20 s) than the peptides exit (77–175 s). We assume that at least partial protonation of the carboxyl groups at the inserted C-terminus would occur, and as a result, a force directed toward the inside of a liposome ($\vec{F}_{in}$) is created. As with insertion, the more charges there are at the C-terminus, the more time it takes for the process of the C-terminus translocation across a bilayer during exit. Our results are consistent with this view, and also confirm our assumption that the peptides exit to the surface of the outside leaflet. Otherwise, if the peptides were able to exit to the inside of a liposome, then the exit rate would not depend on the number of protonatable

residues at the C-terminus; rather, it would be affected by the N-terminus of the peptides and would be highest for pHLIP-4, with fewer charged residues at its N-terminus.

In contrast to other known peptide-based delivery technologies, the selective direct delivery of polar molecules across a membrane by the pHLIP peptide is achieved by the pH-dependent folding and insertion of a monomer across a bilayer, enabling the targeting of acidic tissues. By using variants of the pHLIP peptide and by attaching polar cargoes to the inserting end, we have advanced our understanding of the mechanism of membrane-associated folding/unfolding, providing mechanistic insights on the formation of helical structures and the existence of intermediates, and the mechanism of cargo translocation across the lipid bilayer of a membrane. Here, we summarize the main conclusions:

1. The existence of intermediate states on the folding and unfolding pathways is not mandatory and, in the simple case of a polypeptide with a noncharged and nonpolar inserting end, the folding and unfolding is seen as an all-or-none transition.
2. If the peptide inserting end has charges or a polar cargo attached, an interfacial helical intermediate will occur before a peptide propagates into the hydrophobic core of a membrane.
3. The origin of the driving force for the interfacial helix to insert into a bilayer to adopt a TM orientation might include the distortion of lipids by the partial surface insertion of the peptide. When a polypeptide forms a rigid helical structure and propagates deeply into one monolayer of a lipid bilayer, membrane tension and instability are created (29).
4. A consistent and significant experimental observation is that the formation of secondary structure accompanies the partitioning of a polypeptide into a lipid bilayer, and that peptide exit from a membrane occurs simultaneously with unfolding on this timescale. The energetic cost of breaking backbone H-bonds inside a bilayer appears higher than the cost of the membrane distortion created by an asymmetric inclusion of helices in one leaflet of a membrane lipid bilayer.
5. Our study provides useful principles for the design of drug delivery agents for the translocation of molecules across membranes into the cells in acidic diseased tissues. There are both thermodynamic and kinetic limitations for the direct translocation of polar cargo across membrane by pHLIP. The following parameters correlate inversely with increasing polarity of cargo attached to the peptide inserting end: i), the depth of peptide partitioning onto the membrane surface at neutral pH (state II) that increases the effective concentrations of cargo molecules near the membrane surface; ii), the proportion of peptide molecules in the membrane-inserted state (state III) associated with cargo translocation; and iii), the rate of peptide insertion into a bilayer (transition from state II to III) that moves cargo from the extracellular to the intracellular space.

SUPPORTING MATERIAL

A detailed description of experiments, eight figures, a table, and an appendix are available at http://www.biophysj.org/biophysj/supplemental/S0006-3495(12)00332-3.

We thank Michael Anderson and Dr. Lan Yao for fruitful discussions and comments on the manuscript.

This work was supported by National Institutes of Health grants CA133890 and GM073857 to O.A.A., D.M.E., and Y.R.K., and CA138468 to Y.K.R.

REFERENCES

1. Van den Berg, B., W. M. Clemons, Jr., …, T. A. Rapoport. 2004. X-ray structure of a protein-conducting channel. *Nature.* 427:36–44.
2. Osborne, A. R., T. A. Rapoport, and B. van den Berg. 2005. Protein translocation by the Sec61/SecY channel. *Annu. Rev. Cell Dev. Biol.* 21:529–550.
3. Simpson, P. J., B. Schwappach, …, R. L. Isaacson. 2010. Structures of Get3, Get4, and Get5 provide new models for TA membrane protein targeting. *Structure.* 18:897–902.
4. Brambillasca, S., M. Yabal, …, N. Borgese. 2006. Unassisted translocation of large polypeptide domains across phospholipid bilayers. *J. Cell Biol.* 175:767–777.
5. Renthal, R. 2010. Helix insertion into bilayers and the evolution of membrane proteins. *Cell. Mol. Life Sci.* 67:1077–1088.
6. White, S. H., and W. C. Wimley. 1999. Membrane protein folding and stability: physical principles. *Annu. Rev. Biophys. Biomol. Struct.* 28:319–365.
7. Engelman, D. M., Y. Chen, …, J. L. Popot. 2003. Membrane protein folding: beyond the two stage model. *FEBS Lett.* 555:122–125.
8. Minetti, C. A., and D. P. Remeta. 2006. Energetics of membrane protein folding and stability. *Arch. Biochem. Biophys.* 453:32–53.
9. Urban, S. 2010. Taking the plunge: integrating structural, enzymatic and computational insights into a unified model for membrane-immersed rhomboid proteolysis. *Biochem. J.* 425:501–512.
10. Ladokhin, A. S., and S. H. White. 2004. Interfacial folding and membrane insertion of a designed helical peptide. *Biochemistry.* 43:5782–5791.
11. Reshetnyak, Y. K., M. Segala, …, D. M. Engelman. 2007. A monomeric membrane peptide that lives in three worlds: in solution, attached to, and inserted across lipid bilayers. *Biophys. J.* 93:2363–2372.
12. Reshetnyak, Y. K., O. A. Andreev, …, D. M. Engelman. 2008. Energetics of peptide (pHLIP) binding to and folding across a lipid bilayer membrane. *Proc. Natl. Acad. Sci. USA.* 105:15340–15345.
13. Andreev, O. A., A. D. Dupuy, …, Y. K. Reshetnyak. 2007. Mechanism and uses of a membrane peptide that targets tumors and other acidic tissues in vivo. *Proc. Natl. Acad. Sci. USA.* 104:7893–7898.
14. Musial-Siwek, M., A. Karabadzhak, …, D. M. Engelman. 2010. Tuning the insertion properties of pHLIP. *Biochim. Biophys. Acta.* 1798:1041–1046.
15. Reshetnyak, Y. K., O. A. Andreev, …, D. M. Engelman. 2006. Translocation of molecules into cells by pH-dependent insertion of a transmembrane helix. *Proc. Natl. Acad. Sci. USA.* 103:6460–6465.
16. An, M., D. Wijesinghe, …, D. M. Engelman. 2010. pH-(low)-insertion-peptide (pHLIP) translocation of membrane impermeable phalloidin toxin inhibits cancer cell proliferation. *Proc. Natl. Acad. Sci. USA.* 107:20246–20250.

17. Wijesinghe, D., D. M. Engelman, …, Y. K. Reshetnyak. 2011. Tuning a polar molecule for selective cytoplasmic delivery by a pH (low) insertion peptide. *Biochemistry.* 50:10215–10222.

18. Reference deleted in proof.

19. Andreev, O. A., D. M. Engelman, and Y. K. Reshetnyak. 2010. pH-sensitive membrane peptides (pHLIPs) as a novel class of delivery agents. *Mol. Membr. Biol.* 27:341–352.

20. Vāvere, A. L., G. B. Biddlecombe, …, J. S. Lewis. 2009. A novel technology for the imaging of acidic prostate tumors by positron emission tomography. *Cancer Res.* 69:4510–4516.

21. Reshetnyak, Y. K., L. Yao, …, O. A. Andreev. 2011. Measuring tumor aggressiveness and targeting metastatic lesions with fluorescent pHLIP. *Mol. Imaging Biol.* 13:1146–1156.

22. Andreev, O. A., A. G. Karabadzhak, …, Y. K. Reshetnyak. 2010. pH (low) insertion peptide (pHLIP) inserts across a lipid bilayer as a helix and exits by a different path. *Proc. Natl. Acad. Sci. USA.* 107:4081–4086.

23. Barrera, F. N., D. Weerakkody, …, D. M. Engelman. 2011. Roles of carboxyl groups in the transmembrane insertion of peptides. *J. Mol. Biol.* 413:359–371.

24. Elamrani, K., and A. Blume. 1983. Effect of the lipid phase transition on the kinetics of H^+/OH^- diffusion across phosphatidic acid bilayers. *Biochim. Biophys. Acta.* 727:22–30.

25. Kuyper, C. L., J. S. Kuo, …, D. T. Chiu. 2006. Proton permeation into single vesicles occurs via a sequential two-step mechanism and is heterogeneous. *J. Am. Chem. Soc.* 128:3233–3240.

26. Petkova, A. T., J. G. Hu, …, J. Herzfeld. 1999. Arginine activity in the proton-motive photocycle of bacteriorhodopsin: solid-state NMR studies of the wild-type and D85N proteins. *Biochemistry.* 38:1562–1572.

27. Harris, T. K., and G. J. Turner. 2002. Structural basis of perturbed pKa values of catalytic groups in enzyme active sites. *IUBMB Life.* 53:85–98.

28. Kawase, Y., M. Tanio, …, H. Saitô. 2000. Alteration of conformation and dynamics of bacteriorhodopsin induced by protonation of Asp 85 and deprotonation of Schiff base as studied by ^{13}C NMR. *Biochemistry.* 39:14472–14480.

29. Bohinc, K., D. Lombardo, …, A. Iglic. 2006. Shape variation of bilayer membrane daughter vesicles induced by anisotropic membrane inclusions. *Cell. Mol. Biol. Lett.* 11:90–101.